Research Square

Preprints are preliminary reports that have not undergone peer review.
They should not be considered conclusive, used to inform clinical practice,
or referenced by the media as validated information.

Anterior Cingulate Cortex Metabolism, Microstructure, and Social Withdrawal in Autism Spectrum Disorder

Manabu Makinodan

manabumakinodan@kumamoto-u.ac.jp

Kumamoto University https://orcid.org/0000-0003-4339-9413

Masato Takahashi

Kumamoto University https://orcid.org/0000-0003-3265-0166

Natsuko Kashida

Kumamoto University https://orcid.org/0009-0007-7443-1240

Kiwamu Matsuoka

Rio Ishida

Michihiro Toritsuka

Tsutomu Takeda

Takahiro Yoshihara

Kazuhiko Yamamuro

Nara Medical University https://orcid.org/0000-0002-4362-3262

Hiroto Tamakoshi

Yuhei Takado

National Institutes for Quantum and Radiological Science and Technology https://orcid.org/0000-0001-7484-8424

Article

Keywords:

Posted Date: November 23rd, 2026

DOI: https://doi.org/10.21203/rs.3.rs-11508121/v1

License: This work is licensed under a Creative Commons Attribution 4.0 International License. Read Full License

Additional Declarations: The authors have declared there is **NO** conflict of interest to disclose

Abstract

The anterior cingulate cortex (ACC) supports social behavior, which can be normalized by manipulating ACC function in animal models of autism spectrum disorder (ASD). How ACC metabolism and microstructure jointly relate to social behavior in humans with ASD remains unclear. Proton magnetic resonance spectroscopy measured glutamate (Glu), glutamine (Gln), lactate (Lac), and myo-inositol (Ins), while neurite orientation dispersion and density imaging estimated neurite density index (NDI) and orientation dispersion index (ODI) in the same ACC voxel in 96 adults with ASD and 63 typically developing controls (TDC). Analyses included group comparisons, partial correlations, networks, and permutation-based dimensional models incorporating Japanese Autism-Spectrum Quotient (AQ-J), 25-item Hikikomori Questionnaire (HQ-25), and diagnosis, plus an ASD-only sensitivity analysis using the validated HQ-25 cutoff. ACC Lac was higher in ASD, but the difference was not significant after multiple-comparison correction; Glu, Gln, and Ins did not differ significantly between groups. Four network edges were retained in ASD, with bootstrap support for Glu–Ins and Gln–Lac; none were retained in TDC. Glu correlated significantly with lower NDI and higher ODI only in ASD. HQ-25—but neither AQ-J nor diagnosis—showed significant positive associations with Lac, Glu, and Gln. The ASD-only sensitivity analysis corroborated the Lac association. Altered ACC metabolic–structural coupling in ASD, possibly reflecting astrocytic dysfunction, may be informative beyond concentration differences alone. Metabolite associations with social withdrawal, independent of general autistic traits, suggest a behavioral dimension relevant to precision medicine in ASD.

1 Introduction

Autism spectrum disorder (ASD) is a neurodevelopmental condition characterized by social communication difficulties and restricted, repetitive behavior; its prevalence has increased [1, 2]. Beyond core diagnostic features, social difficulties can manifest as severe isolation in adulthood. Using National Longitudinal Transition Study data, Orsmond et al. found that approximately 40% of adults with autism never saw friends, 47% were never contacted by friends, and 28% were completely socially isolated—proportions markedly higher than among young people with other disabilities [3]. Such isolation may itself affect the brain: in mice, juvenile social isolation alters the function of medial prefrontal pyramidal cells [4]. In a Japanese regional survey, 34.4% of adults with autism without intellectual disability were unemployed and living at home [5].

The anterior cingulate cortex (ACC) plays a central role in social pain processing, emotion regulation, and behavioral inhibition; its activity increases during social exclusion and correlates positively with self-reported distress [6]. As a hub of the social brain network, the ACC has extensive anatomical and functional connections to regions involved in social information processing [7, 8], and altered frontolimbic connectivity including the ACC has been reported in ASD [9, 10]. Metabolic abnormalities of the ACC have also been reported in ASD, and our group has previously shown, using the same MRS approach, that lower ACC taurine levels in children with ASD were associated with restricted and repetitive behaviors but not with social affect [11], indicating that ACC metabolic alterations may relate to specific clinical dimensions. Studies of *Shank3* mutant mice, a validated genetic model of autism, identified ACC dysfunction as a neural substrate of social deficits [12], suggesting that the functional and metabolic state of this region can influence social behavior.

Four interrelated metabolites—glutamate (Glu), glutamine (Gln), lactate (Lac), and myo-inositol (Ins)—provide a neurobiological rationale for integrated ACC assessment. Glu is the principal excitatory neurotransmitter and is widely used in magnetic resonance spectroscopy (MRS) as an index of excitatory neurotransmission [13]. Astrocytes convert Glu to Gln via glutamine synthetase in the Glu–Gln cycle, a process central to glutamatergic homeostasis [14]. Lac indexes enhanced glycolysis associated with the astrocyte–neuron lactate shuttle [15] and has attracted interest in ASD in relation to mitochondrial dysfunction [16, 17]. Ins is an osmoregulatory compound concentrated in astrocytes and serves as a glial marker [18].

Proton MRS (^{1}H-MRS) noninvasively quantifies brain metabolites in vivo. Elevated cingulate Lac, including in the ACC, has been reported in ASD [19, 20], suggesting enhanced glycolysis secondary to mitochondrial dysfunction. ACC Glu and Gln findings are inconsistent, with both elevations and reductions reported [21–23]. Most studies compare absolute metabolite concentrations between groups, leaving coupling between the Glu–Gln cycle and glycolysis insufficiently examined. Abnormal

Glu–Gln cycle enzyme activity in postmortem ACC tissue from individuals with autism [24] raises the possibility that ASD-related abnormalities involve inter-metabolite coupling rather than absolute concentrations. Selective associations between metabolic and clinical indices also remain insufficiently characterized, leaving uncertain which metabolic abnormalities relate to specific symptoms.

Neurite orientation dispersion and density imaging (NODDI) can assess microstructural correlates of metabolic abnormalities. Based on diffusion magnetic resonance imaging (MRI), NODDI separately quantifies the neurite density index (NDI) and orientation dispersion index (ODI), capturing microstructural change with greater sensitivity than diffusion tensor imaging [25]. Glu overactivity can cause excitotoxic neurite loss [26]; together with the miswiring hypothesis of ASD [27], this suggests that ACC metabolic abnormalities may be reflected in NDI and ODI. However, few studies have combined MRS and NODDI at the same ACC location.

Hikikomori is severe social withdrawal persisting for 6 months or longer [28, 29]. Approximately 41% of patients with autism met hikikomori criteria [30], and about 46% of individuals with suspected ASD exceeded the risk cutoff on the 25-item Hikikomori Questionnaire (HQ-25) [31]. The HQ-25 is a validated measure of social withdrawal and avoidance [32], and hikikomori status in ASD can be independent of autistic-trait severity measured by the Autism-Spectrum Quotient (AQ) [30]. Our group has shown in mice that juvenile social deprivation alters medial prefrontal development and persistently reduces adult sociability [33], implicating medial frontal circuits in social behavior. Clarifying how ACC metabolism and microstructure relate to social withdrawal is therefore relevant both to pathophysiology and to clinical support.

Integrated assessment of ACC metabolites (Glu, Gln, Lac, Ins) and NODDI indices (NDI, ODI) within the same region may clarify their links to social withdrawal (HQ-25) in ASD, yet, to our knowledge, no study has examined these indices simultaneously. We therefore acquired them in individuals with ASD (N = 96) and typically developing controls (TDC; N = 63) with three aims: first, to compare ACC metabolic and microstructural indices between groups; second, to compare inter-metabolite and metabolite–NDI/ODI correlation patterns to examine ASD-related metabolic–structural associations; third, to evaluate relationships between these indices and general autistic traits, measured with the Japanese version of the Autism-Spectrum Quotient (AQ-J), and social withdrawal (HQ-25). We hypothesized that a network-level abnormality in metabolic and structural indices centered on the ACC glutamatergic system may underlie social withdrawal in ASD.

2 Materials and methods

2.1 Participants

We recruited adults (aged ≥ 18 years) with ASD receiving outpatient or inpatient care at the Department of Psychiatry, Nara Medical University Hospital. At least two trained psychiatrists or psychologists diagnosed ASD according to the Diagnostic and Statistical Manual of Mental Disorders, Fifth Edition [34], and inclusion required meeting the Autism Diagnostic Observation Schedule, Second Edition (ADOS-2), Module 4 classification criteria [35, 36]. The Mini-International Neuropsychiatric Interview (MINI) screened for psychiatric comorbidities [37]; individuals with major psychiatric disorders or suicidal ideation were excluded. Intellectual functioning was estimated using an abbreviated two-subtest battery of the Wechsler Adult Intelligence Scale, Fourth Edition (WAIS-IV; Similarities and Symbol Search), with scores prorated to an estimated full-scale intelligence quotient (FSIQ) using the Tellegen and Briggs procedure [38]. Participants with an estimated full-scale intelligence quotient (FSIQ) < 70 were excluded because the study focused on ASD without intellectual disability. The final ASD sample comprised 96 individuals (64 males, 32 females) with scores ≥ 26 on the Japanese version of the Autism-Spectrum Quotient (AQ-J) [39].

TDC were recruited through local print advertisements and assessed by two experienced psychiatrists, including psychiatric evaluation and medical history review. As in the ASD group, the MINI was administered, and individuals with major psychiatric disorders, suicidal ideation, an AQ-J score ≥ 26, or an estimated FSIQ < 70 were excluded. The final TDC sample comprised 63 individuals with no history or current diagnosis of ASD, psychiatric disorders, or neurological conditions. Comorbidities and

medication use in the ASD group are summarized in Supplementary Tables 1 and 2, and participant flow is shown in Supplementary Fig. 1.

2.2 Assessment of autistic traits

Autistic traits were assessed using the self-report AQ-J, allowing direct comparisons between the ASD and TDC groups. The ADOS-2 was administered only to individuals with ASD to confirm diagnosis, whereas the AQ-J provided a standardized measure of autistic traits across all participants [39, 40].

2.3 Assessment of hikikomori traits

Hikikomori traits were assessed using the HQ-25, a self-report scale evaluating social withdrawal over the past 6 months. All participants completed the questionnaire to allow standardized comparisons across groups. Its 25 items use a 5-point Likert scale (0 = strongly disagree, 4 = strongly agree). Specific items (e.g., those concerning social motivation) are reverse-scored so that higher total scores indicate greater hikikomori risk. The original validation study established a cutoff score of 42, with scores of 42 or higher used to identify individuals at risk [32].

2.4 MRI acquisition

MRI and MRS examinations used a 3 T scanner (Siemens MAGNETOM Skyra, Erlangen, Germany) with a 32-channel receiver head coil. Three-dimensional T1-weighted gradient-echo images comprised gapless sagittal sections (repetition time [TR] = 2 500 ms; echo time [TE] = 2.18 ms; inversion time = 1 000 ms; field of view = 256 mm; flip angle = 8°; acquisition matrix = 320 × 300; slice thickness = 0.8 mm).

2.4.1 MRS acquisition

The ACC voxel of interest (VOI; 30 × 20 × 20 mm^3) was placed on the anatomical images (Fig. 1a). As in previous studies [41, 42], a short-TE spin-echo full-intensity acquired localized (SPECIAL) single-voxel sequence [43] was used (TE = 8.5 ms, TR = 3 000 ms, 128 averages).

2.4.2 Diffusion MRI acquisition for NODDI

NODDI used a two-shell echo-planar diffusion protocol (TR = 3,600 ms; TE = 90 ms; b = 0, 700, and 2,000 s/mm^2; matrix = 120 × 120; flip angle = 90°). Diffusion-weighted images were acquired in two runs with opposite phase-encoding directions (anterior-to-posterior, 67 volumes; posterior-to-anterior, 68 volumes), enabling susceptibility-distortion correction.

2.4.3 MRS data analysis

Spectra were preprocessed (coil combination, rejection of motion-corrupted averages, and frequency and phase correction) using FID-A in MATLAB 2021a (MathWorks, Natick, MA, USA) [44] and fitted with LCModel version 6.3-1R (Stephen Provencher, Oakville, ON, Canada) [45, 46], using a basis set that included nine macromolecular functions [41] (Fig. 1b). Metabolite concentrations (mmol/L) were referenced to tissue water and corrected for tissue composition and relaxation [47–49], with tissue fractions from FSL FAST [50] (Supplementary Methods). The MRSinMRS checklist is in Supplementary Table 3 [51].

2.4.4 NODDI data analysis

Diffusion-weighted images were processed using FSL version 6.0.6.2 (FMRIB Center, Department of Clinical Neurology, University of Oxford, Oxford, England; http://www.fmrib.ox.ac.uk/fsl/) [52]. Susceptibility-induced off-resonance fields were estimated with TOPUP using paired images acquired with reversed phase-encoding blips [53]. TOPUP distortion correction was followed by eddy-current and motion correction using FSL eddy [54]. The NODDI model was fitted with toolbox version 1.01 (https://www.nitrc.org/projects/noddi_toolbox/) running in MATLAB 2021a (MathWorks, Natick, MA, USA), and ODI and NDI maps were calculated.

NODDI regions of interest (ROIs) were derived from the ACC MRS VOIs placed by an experienced MRI technician at the time of MRS acquisition (Fig. 1a). This ensured spatial correspondence between metabolite measurements and microstructural indices. Each participant's NDI and ODI maps were coregistered to the three-dimensional T1-weighted image. Regional values were calculated by averaging all voxels within the ACC ROI, which encompassed gray matter and underlying white matter because of the MRS voxel's spatial extent.

2.5 Statistical data analysis

Analyses used IBM SPSS Statistics version 28 (IBM Corp., Armonk, NY) and R version 4.5.1 (R Foundation for Statistical Computing, Vienna, Austria; 2026). Group characteristics were compared using Mann–Whitney U tests for continuous variables, including nonnormally distributed data, and chi-square tests for categorical variables.

Because FSIQ differed between groups, permutation-based one-way analysis of covariance (ANCOVA) compared each MRS and NODDI index using the Freedman–Lane method (5,000 permutations), adjusting for age, sex, and FSIQ.

To test whether ACC metabolite associations with social withdrawal were independent of general autistic traits or diagnosis, we fitted separate dimensional general linear models for Lac, Glu, Gln, and Ins. AQ-J score, HQ-25 score, and diagnostic group (ASD/TDC) were predictors of interest; age, sex, and FSIQ were covariates. AQ-J and HQ-25 total scores were mean-centered across the full sample before model fitting. Variance inflation factors (VIFs) were inspected to assess multicollinearity against the threshold VIF < 5. Models used the same permutation-based approach described above. For each metabolite, an additional model included a Diagnosis × HQ-25 interaction to examine whether the association differed by diagnostic group.

Following group comparisons, partial correlations were calculated within each cohort to examine relationships among metabolic, microstructural, and clinical indices. To address nonnormality while controlling for age, sex, and FSIQ, we calculated Spearman rank partial correlation coefficients. Variables were first residualized using linear regression with these covariates; the residuals were then ranked and correlated. We first examined associations among metabolites, followed by relationships between metabolites and NODDI indices. For clinical subgroup comparisons, participants were stratified using the established HQ-25 cutoff of 42 [32]. An ASD-only sensitivity analysis compared ACC Lac between participants at or above versus below the cutoff using the same permutation-based ANCOVA. This analysis tested the primary Lac hypothesis and was restricted to Lac, identified a priori as the primary outcome.

To integrate metabolic and microstructural associations, we estimated separate ASD and TDC partial correlation networks for six ACC variables: Glu, Gln, Lac, Ins, NDI, and ODI. All variables were first residualized for age, sex, and FSIQ using linear regression. Sparse networks were constructed from Spearman partial correlations using EBICglasso with $\gamma = 0.25$. The default $\gamma = 0.5$ yielded an empty network at the current sample sizes (ASD: n = 96; TDC: n = 63). The use of $\gamma = 0.25$ is consistent with recommendations for small-to-moderate samples [55]. Edge-weight stability was assessed using nonparametric bootstrapping (1,000 iterations) to obtain 95% confidence intervals (CIs); edges with CIs excluding zero were considered stable. Case-dropping bootstrapping (1,000 iterations) yielded correlation stability (CS) coefficients for centrality indices, which were interpreted only if ≥ 0.25. All network analyses used bootnet and qgraph in R.

A supplementary analysis assessed potential medication confounding of the ACC Lac group difference by adding benzodiazepine use, attention-deficit/hyperactivity disorder (ADHD) medication use, and antipsychotic use as covariates.

For all tests, significance was set at $p < 0.05$. False discovery rate (FDR) correction was applied to account for multiple comparisons in ASD–TDC comparisons of MRS metabolites, dimensional models relating AQ-J, HQ-25, and diagnosis to each metabolite, and the correlation analyses.

3 Results

3.1 Demographic and clinical characteristics

Group characteristics were compared in ASD (64 males, 32 females) and TDC (35 males, 28 females). Neither age ($p = 0.84$, $U = 2967.00$) nor sex distribution ($p = 0.16$, $\chi^2 = 1.99$) differed significantly between groups (Table 1). FSIQ was significantly lower in ASD than in TDC ($p = 6.90 \times 10^{-4}$, $U = 2060.50$) (Table 1). Regarding clinical measures, participants with ASD had significantly higher total scores on AQ-J ($p = 1.62 \times 10^{-24}$, $U = 124.00$, $r = 0.81$) and HQ-25 ($p = 4.45 \times 10^{-19}$, $U = 490.00$, $r = 0.71$) (Table 1). Group differences were also significant across all subscales. AQ-J social skills, attention switching, communication, imagination, and local details scores were higher in ASD (all $p < 0.05$). HQ-25 socialization, isolation, and emotional support scores were higher in ASD, whereas motivation scores were lower than in TDC (all $p < 0.001$). These results indicate a high burden of clinical symptoms and substantial social-communicative difficulties in the ASD sample.

Table 1
Demographic and clinical characteristics of the ASD and TDC groups.

	ASD			**TDC**			**Statistics**		
	N = 96 (64/32)			**N = 63 (35/28)**			**χ^2 = 1.99 (p = 0.16)**		
	Mean	SD	Median	Mean	SD	Median	U	p	r
Age, years	27.88	6.58	27.50	27.73	6.93	27.00	2967.00	0.84	0.02
Estimated FSIQ	96.95	13.88	97.16	103.53	10.20	103.07	2060.50	6.90×10^{-4}	0.27
AQ-J total	31.52	6.36	32.00	14.43	4.42	14.00	124.00	1.62×10^{-24}	0.81
AQ-J: social skill	6.98	2.44	7.00	2.19	1.86	2.00	461.00	1.23×10^{-19}	0.72
AQ-J: attention switching	7.22	1.63	8.00	3.73	1.74	4.00	484.50	1.97×10^{-19}	0.71
AQ-J: local details	5.09	2.11	5.00	4.37	1.90	4.00	2430.00	3.44×10^{-2}	0.18
AQ-J: communication	6.81	2.06	7.00	1.44	1.45	1.00	193.00	1.03×10^{-23}	0.80
AQ-J: imagination	5.42	2.11	6.00	2.70	1.64	3.00	994.50	5.71×10^{-13}	0.57
HQ-25 total	56.77	18.04	59.00	24.19	11.71	22.00	490.00	4.45×10^{-19}	0.71
HQ-25: socialization	28.04	8.81	29.50	13.05	6.75	13.00	552.50	3.07×10^{-18}	0.69
HQ-25: isolation	17.82	6.42	19.00	7.56	4.58	7.00	690.00	1.87×10^{-16}	0.65
HQ-25: emotional support	10.91	6.22	11.00	3.59	3.45	3.00	994.00	7.77×10^{-13}	0.57
HQ-25: 25motivation	6.48	4.05	6.50	11.40	2.47	11.00	960.00	3.12×10^{-13}	0.58

Notes: Data are presented as mean, SD, and median unless otherwise indicated. Group differences between the autism spectrum disorder (ASD) and typically developing controls (TDC) groups were examined using the two-sided Mann–Whitney U test. Sex distribution was compared using Pearson's chi-square test. Effect size (r) was calculated as $|Z|/\sqrt{N}$.

Abbreviations: ASD, autism spectrum disorder; TDC, typically developing controls; SD, standard deviation; U, Mann–Whitney U statistic; r, effect size; FSIQ, full-scale intelligence quotient; AQ-J, Japanese version of the Autism-Spectrum Quotient; HQ-25, 25-item Hikikomori Questionnaire.

3.2 Comparison of metabolite concentrations and diffusion indices

Group comparisons used linear models with diagnosis as the primary factor, adjusting for age, sex, and estimated FSIQ. Lac concentrations were higher in ASD than in TDC before multiple-comparison correction (B = 0.087, p = 0.013, 95% CI [0.017, 0.157]; Table 2). The FDR-corrected q value across four MRS indices was 0.052, which did not meet the significance threshold. No significant group differences were observed for Glu (p = 0.272), Gln (p = 0.474), or Ins (p = 0.904). The microstructural indices NDI (p = 0.929) and ODI (p = 0.739) also did not differ significantly between groups (Table 2). Detailed model results, including covariate effects, are summarized in Supplementary Table 4. Sex was significantly associated with Glu, Gln, and Lac (all p < 0.05), and age with Lac, Glu, Gln, NDI, and ODI (all p < 0.01). These findings underscore the importance of demographic adjustment when evaluating metabolic and microstructural differences in ASD.

Table 2
Comparison of metabolite concentrations and diffusion indices between ASD and TDC groups adjusted for age, sex, and estimated FSIQ.

Variable	ASD		TDC		Estimate(B)	Permutation p	q†	95% CI		
	Mean	SD	Mean	SD						
MRS indices										
Gln	2.238	0.567	2.143	0.419	0.053	0.474	0.632	-0.093	-	0.200
Glu	10.973	0.569	10.848	0.576	0.101	0.272	0.544	-0.079	-	0.280
Lac	0.903	0.261	0.799	0.146	0.087	**0.013***	0.052	0.017	-	0.157
Ins	7.480	0.655	7.486	0.555	0.013	0.904	0.904	-0.190		0.216
NODDI indices										
NDI	0.451	0.014	0.451	0.016	1.928×10^{-4}	0.929	0.929	-0.004	-	0.004
ODI	0.442	0.013	0.443	0.013	-0.001	0.739	0.929	-0.005	-	0.003

Notes: Group differences between the autism spectrum disorder (ASD) and typically developing controls (TDC) groups were examined using a linear model with permutation tests (5 000 permutations), adjusted for age, sex, and estimated FSIQ. Estimates (B) and their 95% confidence intervals (CI) were calculated from the corresponding linear model; age and estimated FSIQ were z-standardized. * p < .05.

Abbreviations: ASD, autism spectrum disorder; TDC, typically developing controls; Gln, Glutamine; Glu, Glutamate; Lac, Lactate; Ins, myo-inositol; NDI, neurite density index; ODI, Orientation Dispersion Index; SD, standard deviation; p, permutation-based p-value; q†, FDR-corrected q-value (Benjamini-Hochberg); CI, confidence interval; B, unstandardized regression coefficient.

3.3 Inter-metabolite correlations within each cohort

Partial Spearman correlations showed different inter-metabolite association patterns, with more significant correlations in ASD (Supplementary Table 5). Within ASD, Glu correlated positively with Lac (ρ = 0.22, q = 0.0499) and Ins (ρ = 0.41, q = 1.12×10^{-4}), Gln correlated positively with Lac (ρ = 0.42, q = 1.12×10^{-4}), and Lac correlated negatively with Ins (ρ = −0.22, q =

0.0499). Within TDC, only the Glu–Gln correlation was significant (ρ = 0.38, q = 0.012). These associations suggest altered ACC metabolic coupling in ASD involving excitatory neurotransmitter cycling (Glu/Gln), lactate metabolism (Lac), and osmoregulation/glial markers (Ins).

3.4 Neurometabolite–microstructure relationships within each cohort

We examined associations between metabolite concentrations and NODDI-derived microstructural indices within each cohort (Supplementary Table 6). In ASD, Glu correlated negatively with NDI (ρ = −0.316, q = 0.008) and positively with ODI (ρ = 0.311, q = 0.008). The nominal negative correlations of Gln and Lac with NDI did not survive correction (ρ = −0.229 and − 0.222; q = 0.059 for both). In TDC, no metabolite–NODDI correlation survived correction. Glu therefore showed the clearest association with neurite microstructure in ASD.

3.5 Group-specific network topography

EBICglasso network analysis (γ = 0.25) integrated ACC metabolic–microstructural relationships (Fig. 2). Four edges were retained after regularization in ASD (Fig. 2a): Glu–Ins (r = 0.168), Gln–Lac (r = 0.112), Glu–ODI (r = 0.066), and Glu–NDI (r = −0.072). In contrast, no edges were retained in TDC (Fig. 2b). Edge stability was evaluated using nonparametric bootstrapping (1,000 iterations). The 95% CIs for Glu–Ins and Gln–Lac excluded zero, supporting their stability. The remaining two edges, Glu–ODI and Glu–NDI, had wider CIs overlapping zero and warrant caution. The Gln–Lac edge, retained only in ASD, suggests coupling between the Glu–Gln cycle and lactate metabolism, consistent with altered astrocyte–neuron interactions. The Glu–Ins edge also suggests glial involvement, given that Ins is an astrocyte-related marker. Although Glu was partially correlated with NDI and ODI, these network edges were unstable in bootstrap analyses and remain exploratory. Centrality stability was evaluated using case-dropping bootstrapping (1,000 iterations). CS coefficients for strength, closeness, and betweenness were below the recommended threshold of 0.25 in both groups [55]; centrality indices were therefore not interpreted.

3.6 Social withdrawal–metabolite associations in dimensional models

Full-sample models and ASD-only sensitivity analysis

To examine associations of ACC metabolites with autistic traits and social withdrawal, we fitted dimensional models including AQ-J, HQ-25, and diagnosis, adjusting for age, sex, and FSIQ (Table 3). HQ-25 was positively associated with Lac (β = 0.003, 95% CI [0.001, 0.005], p = 0.006), Glu (β = 0.007, [0.002, 0.013], p = 0.014), and Gln (β = 0.007, [0.002, 0.012], p = 0.004), and these associations remained significant after FDR correction (q ≤ 0.019). Neither AQ-J nor diagnosis was associated with any metabolite, and Ins was not associated with any predictor. Variance inflation factors were acceptable (AQ-J, 3.64; diagnosis, 3.68), and no Diagnosis × HQ-25 interaction was significant (all p > 0.05). Only 9.5% of TDC exceeded the HQ-25 cutoff of 42, compared with 80.2% of ASD (χ^2 = 76.17, p < 0.001), so the upper range of HQ-25 was sparsely represented in TDC. In the ASD-only sensitivity analysis, participants at or above the cutoff (n = 77) had higher ACC Lac than those below it (n = 19; β = 0.154, 95% CI [0.032, 0.277], p = 0.014; Fig. 2c).

Table 3
Association between dimensional autism/withdrawal measures and ACC metabolites.

Metabolite	AQ-J	HQ-25	Diagnosis (TDC vs. ASD)
Lac	β = -0.002	**β = 0.003**	β = -0.013
	[-0.008, 0.004]	**[0.001, 0.005]**	[-0.139, 0.113]
	p = 0.601, q = 0.601	**p = 0.006, q = 0.011**	p = 0.836, q = 0.924
Glu	β = -0.009	**β = 0.007**	β = -0.020
	[-0.025, 0.007]	**[0.002, 0.013]**	[-0.345, 0.306]
	p = 0.258, q = 0.517	**p = 0.014, q = 0.019**	p = 0.917, q = 0.924
Gln	β = -0.011	**β = 0.007**	β = -0.012
	[-0.024, 0.002]	**[0.002, 0.012]**	[-0.275, 0.251]
	p = 0.104, q = 0.414	**p = 0.004, q = 0.011**	p = 0.924, q = 0.924
Ins	β = -0.005	β = 0.003	β = -0.025
	[-0.024, 0.013]	[-0.004, 0.009]	[-0.400, 0.349]
	p = 0.562, q = 0.601	p = 0.458, q = 0.458	p = 0.890, q = 0.924

Notes: Values are unstandardized regression coefficients (β; per 1-point increase in AQ-J or HQ-25 score) with 95% confidence intervals (CI), permutation-based p values (5 000 permutations, Freedman–Lane method), and Benjamini–Hochberg false discovery rate (FDR)-adjusted q values, presented as β [95% CI]; p, q. CIs were calculated as the estimate ± 1.96 × standard error. A separate general linear model was fitted for each metabolite, including AQ-J, HQ-25, and diagnosis as predictors and age, sex, and estimated FSIQ as covariates (covariate coefficients not shown). AQ-J and HQ-25 total scores were mean-centered across the full sample. Variance inflation factors were 3.64 for AQ-J, 2.38 for HQ-25, and 3.68 for diagnosis. Diagnosis coefficients represent TDC relative to ASD. FDR correction was applied separately for each predictor across the four metabolites. Bold values indicate associations that remained significant after FDR correction ($q < 0.05$).

Abbreviations: Lac, lactate; Glu, glutamate; Gln, glutamine; Ins, myo-inositol; AQ-J, Japanese version of the Autism-Spectrum Quotient; HQ-25, 25-item Hikikomori Questionnaire; ASD, autism spectrum disorder; TDC, typically developing controls; ACC, anterior cingulate cortex; FSIQ, full-scale intelligence quotient; FDR, false discovery rate.

3.7 Medication status and ACC Lac

A general linear model examined the ACC Lac group difference after adjustment for age, sex, FSIQ, benzodiazepine use, ADHD medication use, and antipsychotic use (Table 4). Lac was significantly higher in ASD than in TDC (B = 0.080, permutation p = 0.045). Age (B = 0.060, permutation p = 0.001) and male sex (B = 0.074, permutation p = 0.037) were positively associated with Lac. Participants not receiving ADHD medication had significantly higher Lac than those receiving it (B = − 0.186, permutation p = 0.013), suggesting a possible pharmacological influence on ACC lactate metabolism. Neither benzodiazepine use (B = 0.081, permutation p = 0.078) nor antipsychotic use (B = 0.011, permutation p = 0.853) was significantly associated with Lac.

Table 4
ACC lactate concentration by diagnosis after adjustment for age, sex, estimated FSIQ, and medication use.

Predictor	Estimate (B)	Permutation p	95% CI		
Group (ASD)	0.080	**0.045***	0.002	-	0.158
Age	0.060	**0.001****	0.026	-	0.093
Estimated FSIQ	-0.009	0.595	-0.043	-	0.024
Sex (male)	0.074	**0.037***	0.005	-	0.142
Benzodiazepine use	0.081	0.078	-0.009	-	0.171
ADHD medication use	-0.186	**0.013***	-0.324	-	-0.049
Antipsychotic use	0.011	0.853	-0.102	-	0.123

Notes: Permutation p-values were derived from 5 000 permutation iterations. Reference categories were TDC for group, female for sex (male = 1), and non-use for benzodiazepine, ADHD medication, and antipsychotic use. Estimates (B) and their 95% confidence intervals (CI) were calculated from the corresponding linear model; age and estimated FSIQ were z-standardized. * $p < 0.05$, ** $p < 0.01$.

Abbreviations: ACC, anterior cingulate cortex; ADHD, attention-deficit/hyperactivity disorder; CI, confidence interval; FSIQ, full-scale intelligence quotient; Lac, lactate.

4 Discussion

We examined ACC metabolic and microstructural abnormalities in ASD and their clinical correlates. ACC Lac was higher in ASD, but not after FDR correction, and Glu, Gln, and Ins did not differ between groups. Nevertheless, ASD showed a different pattern of ACC metabolic coupling not seen in TDC. Glu also correlated significantly with lower NDI and higher ODI only in ASD, suggesting metabolic–microstructural coupling. Metabolite concentrations were associated with social withdrawal (HQ-25) independently of general autistic traits (AQ-J) and diagnosis. Altered ACC metabolic–microstructural coupling, plausibly reflecting astrocytic dysfunction, may thus be informative beyond concentration differences.

Although the ACC Lac difference did not survive FDR correction, its direction agrees with previous reports of elevated cingulate Lac in autism [19, 20]. Elevated brain lactate and reduced pH were also found across animal models of psychiatric illness, including autism, after accounting for potential confounders [56], consistent with the possibility that our finding reflects metabolic changes rather than confounding alone. The stable Gln–Lac network edge further supports altered Lac-related coupling in ASD.

Glu, Gln, and Ins concentrations did not differ significantly between groups. Previous MRS studies in autism reported elevated ACC Glu [21, 22] or reductions [23]. This inconsistency may reflect differences in participant age, MRS sequence, voxel placement, and covariate adjustment. Here, sex was significantly associated with both Glu and Gln, suggesting that adjustment for sex may partly explain divergent findings. Other studies found reduced ACC Ins in children with Asperger syndrome [57] or no significant group difference in Ins [23, 58]; findings across studies therefore remain inconsistent.

Despite similar concentrations, inter-metabolite coupling differed between groups. Glu and Gln correlated positively in TDC but not in ASD, whereas in ASD, Glu correlated positively with Lac and Ins, Gln with Lac, and Lac negatively with Ins; the regularized network retained four edges in ASD but none in TDC (the TDC Glu–Gln correlation did not survive regularization). ACC metabolic abnormalities in ASD may therefore involve altered coupling among metabolic pathways rather than static concentration differences alone, and the Gln–Lac and Glu–Ins edges are consistent with astrocytic dysfunction. Under physiological conditions, Gln production is regulated relatively independently of glycolysis and lactate production [14], so their coupling in ASD suggests that Glu–Gln cycling may be pathologically coupled to enhanced glycolysis, consistent with

abnormal Glu–Gln cycle enzyme activity in postmortem ACC tissue from individuals with autism [24]. Ins is an astrocyte-related marker [18], and Glu–Ins covariation may reflect an exaggerated astrocytic response to synaptic glutamate accumulation; concurrent ACC Glu, Gln, and Ins elevations with a Gln–Ins correlation only in ASD have also been reported in adults with autism [22].

In ASD, higher Glu co-occurred with lower NDI and higher ODI, suggesting differences in both neurite density and organization, whereas neither correlation was significant in TDC. This raises the possibility of an ASD-related process, although these associations are not evidence of progressive neurite loss.

The Glu–NDI and Glu–ODI edges had bootstrap CIs including zero and remain exploratory, although their directions agreed with the individual correlations. In Shank3 mutant mice, reduced synapse numbers and impaired synaptic transmission in ACC pyramidal neurons produced circuit dysfunction and social deficits [12], and lower NDI may correspondingly reflect lower synaptic and neurite density in the human ACC [59]. Higher ODI is compatible with disorganized neurite trajectories, but ODI is also sensitive to glial density, including microglia [60], so a glial contribution cannot be excluded. Our group previously showed in vitro that cytokines secreted by macrophages derived from adults with ASD shorten and simplify the dendrites of human excitatory neurons [61], suggesting an immune-related route to these microstructural patterns.

Chronic glutamate excess can cause dendritic retraction through excitotoxicity [26], whereas, under the miswiring hypothesis of autism [27], structural circuit inefficiency could drive compensatory Glu upregulation. These directions are not mutually exclusive and may reinforce each other, but cross-sectional correlations cannot establish causal direction.

Matching the MRS voxel and NODDI ROI to the same ACC location enabled spatially corresponding comparisons, but because both techniques sample the same heterogeneous tissue through different physical principles, the observed coupling may reflect the same cellular population seen by each method and cannot be assigned to a specific cell type. Two findings suggest that shared sampling alone does not explain it: only Glu-related microstructural associations survived regularization, whereas those involving Lac, Gln, and Ins did not; and the Glu–NDI and Glu–ODI correlations were present only in ASD although the voxel–ROI overlap was identical in TDC. Nevertheless, differences in statistical power or an ASD-specific confound affecting Glu could contribute to this selectivity.

A central question is which clinical dimension relates to these ACC findings. Elevated lactate may reflect enhanced glycolysis secondary to mitochondrial dysfunction [16, 17], yet previous studies have not found significant correlations between lactate and clinical measures of autistic traits. In our dimensional models, HQ-25, but neither AQ-J nor diagnosis, was positively associated with Lac, Glu, and Gln, identifying social withdrawal severity as a candidate dimensional correlate of ACC metabolism beyond general autistic-trait severity or categorical diagnosis.

The Diagnosis × HQ-25 interaction was not significant, but few TDC scored highly on HQ-25, so limited data at the upper end may obscure group differences rather than establish equivalent effects. The diagnosis-adjusted associations suggest that ACC metabolic alterations could be shared across individuals with social withdrawal rather than specific to autism, a potentially transdiagnostic hypothesis that requires testing in other populations with social withdrawal. Within ASD, where HQ-25 scores spanned a wider range, higher ACC Lac in participants at or above the cutoff agreed with the continuous analysis.

Autism encompasses substantial neurobiological heterogeneity, and resolving this heterogeneity is important for precision medicine [62]. A subgroup characterized by mitochondrial dysfunction has been identified [17, 63], and continuous social withdrawal severity may capture aspects of metabolic heterogeneity beyond the binary distinction of diagnosis. If so, HQ-25 could serve as a clinical index for stratifying neurobiological heterogeneity within autism.

These associations may inform hypotheses about repetitive transcranial magnetic stimulation (rTMS) in autism. Left dorsolateral prefrontal cortex (DLPFC) rTMS has been reported to improve executive function, repetitive behavior, and social functioning [64, 65], and in a randomized controlled trial it changed combined Glu and Gln (Glx) levels in a baseline-dependent, normalizing manner [66]. Its metabolic effects can extend to remote regions, including the cingulate cortex [67], possibly via DLPFC–ACC functional connectivity [68]. In a mouse model of Alzheimer's disease, rTMS increased expression of the

astrocytic glutamate transporter EAAT2/GLT-1, enhancing glutamate clearance and reducing excitotoxicity [69], and a similar EAAT-mediated mechanism has been proposed in children with autism [70]. rTMS might therefore alleviate ACC metabolic vulnerability by restoring astrocytic glutamate reuptake.

Enhancing ACC activity, restoring ACC Shank3 expression, or applying a positive AMPA receptor modulator improved social behavior in Shank3 mutant mice [12], and the metabolite associations observed here were with HQ-25 independently of AQ-J. Normalizing ACC metabolism might therefore target social withdrawal rather than core diagnostic features. However, few MRS studies have examined ACC metabolism after DLPFC rTMS in autism, and none has assessed HQ-25. Longitudinal studies combining pre- and post-rTMS ACC MRS, NODDI, and HQ-25 are needed.

In summary, ACC Lac did not differ significantly between groups after correction, but ASD showed distinct patterns of metabolic coupling and Glu–microstructure associations not observed in TDC. Independent of general autistic traits, metabolite associations with social withdrawal suggest a behavioral dimension relevant to precision medicine in ASD. Longitudinal and interventional studies combining ACC MRS, NODDI, and HQ-25 are needed to test these possibilities; if confirmed, ACC metabolic and structural alterations may represent a target for intervention against social withdrawal in ASD.

5 Limitations

This study has some limitations. First, the cross-sectional design precludes causal inference; longitudinal studies combining MRS and NODDI are needed to determine whether metabolic abnormalities precede, follow, or develop in parallel with microstructural changes. Second, AQ-J and diagnosis overlap conceptually, which may have reduced power to detect their independent effects, and the groups differed in FSIQ, which linear adjustment may not fully account for. The substantial sex effects also warrant sex-stratified analyses. Third, psychotropic medication could not be fully controlled: 59 of 96 participants with ASD (61.5%) received one or more psychotropic medications (Supplementary Table 2). Non-use of ADHD medication was associated with higher Lac (Table 4), but the design cannot distinguish pharmacological effects from comorbid ADHD, and type, dose, and duration were not controlled. Validation in medication-naïve ASD cohorts is needed. Fourth, network centrality CS coefficients were below 0.25 in both groups, likely reflecting sample size, so interpretation focused on edge weights. Fifth, AQ-J and HQ-25 are self-report measures and may be affected by limited introspection. The ASD sample comprised adults seeking clinical care and excluded individuals with more severe withdrawal not accessing care, and the HQ-25 associations were derived from a two-group ASD–TDC comparison, so generalization to other populations with social withdrawal requires further investigation.

Declarations

Data availability

Data are available from the corresponding author upon reasonable request.

Acknowledgements

We sincerely thank all the participants in this study.

Funding

This work was supported by KAKENHI (JP24K02386 to M.M.); the Japan Agency for Medical Research and Development (AMED; grant numbers 24gm1910004h0002, 24gm1510009s0103, 25wm0625510s0102 and JP25wm0625126 to M.M.); Moonshot R&D (grant number JPMJMS239F-1-2 to M.M.), and JSPS Program for Forming J-PEAKS (JPJS00420240025).

Author contributions

N.K. and Ma.T. contributed to data collection, data analysis, and manuscript writing. K.M. contributed to data collection and analysis. R.I. contributed to data collection. Mi.T., K.Y., T.T., H.T., and T.Y. contributed to data analysis. Y.T. contributed to data analysis and provided technical guidance. M.M. contributed to data analysis and manuscript writing.

Conflict of Interest

The authors declare no competing interest.

Ethics approval and informed consent

All experimental procedures were conducted in accordance with the relevant guidelines and regulations. The clinical component of this study was reviewed and approved by the Ethics Committee of Nara Medical University (approval No. 1319). Written informed consent was obtained from all participants prior to their inclusion in the study.

References

1. Shaw KA, Maenner MJ, Baio J, Washington A, Christensen DL, Wiggins LD, et al. Early Identification of Autism Spectrum Disorder Among Children Aged 4 Years — Early Autism and Developmental Disabilities Monitoring Network, Six Sites, United States, 2016. MMWR Surveill Summ. 2020;69:1–11. https://doi.org/10.15585/mmwr.ss6903a1
2. Zeidan J, Fombonne E, Scorah J, Ibrahim A, Durkin MS, Saxena S, et al. Global prevalence of autism: A systematic review update. Autism Res. 2022;15:778–90. https://doi.org/10.1002/aur.2696
3. Orsmond GI, Shattuck PT, Cooper BP, Sterzing PR, Anderson KA. Social Participation Among Young Adults with an Autism Spectrum Disorder. J Autism Dev Disord. 2013;43:2710–9. https://doi.org/10.1007/s10803-013-1833-8
4. Nishihata Y, Yoshino H, Ogawa Y, Sugimura T, Okamura K, Kimoto S, et al. Effect of juvenile social isolation on excitability of prefrontal pyramidal cells with different subcortical axonal projections. Front Cell Neurosci. 2025;19:1549352. https://doi.org/10.3389/fncel.2025.1549352
5. Watanabe H, Koyano Y, Yamashina M. Analysis of Problems Concerning Support for Persons with Autistic Spectrum Disorder and without Intellectual Disabilities at Community-based Facilities for Persons with Disabilities. Journal of Health Care and Nursing. 2016;12:11–7. https://doi.org/10.60254/jhcn.12.2_11
6. Eisenberger NI, Lieberman MD, Williams KD. Does Rejection Hurt? An fMRI Study of Social Exclusion. Science. 2003;302:290–2. https://doi.org/10.1126/science.1089134
7. Apps MAJ, Rushworth MFS, Chang SWC. The Anterior Cingulate Gyrus and Social Cognition: Tracking the Motivation of Others. Neuron. 2016;90:692–707. https://doi.org/10.1016/j.neuron.2016.04.018
8. Holroyd CB, Yeung N. Motivation of extended behaviors by anterior cingulate cortex. Trends Cogn Sci. 2012;16:122–8. https://doi.org/10.1016/j.tics.2011.12.008
9. Delmonte S, Gallagher L, O'Hanlon E, McGrath J, Balsters JH. Functional and structural connectivity of frontostriatal circuitry in Autism Spectrum Disorder. Front Hum Neurosci. 2013;7:430. https://doi.org/10.3389/fnhum.2013.00430
10. Guo Z, Tang X, Xiao S, Yan H, Sun S, Yang Z, et al. Systematic review and meta-analysis: multimodal functional and anatomical neural alterations in autism spectrum disorder. Mol Autism. 2024;15:16. https://doi.org/10.1186/s13229-024-00593-6
11. Minami A, Matsuoka K, Takahashi M, Ueda K, Ohnishi H, Fujimoto Y, et al. Association between decreased taurine levels in the anterior cingulate cortex and restricted and repetitive behaviors in autism spectrum disorder: a cross-sectional

study. Front Psychiatry. 2025;16:1700059. https://doi.org/10.3389/fpsyt.2025.1700059

12. Guo B, Chen J, Chen Q, Ren K, Feng D, Mao H, et al. Anterior cingulate cortex dysfunction underlies social deficits in Shank3 mutant mice. Nat Neurosci. 2019;22:1223–34. https://doi.org/10.1038/s41593-019-0445-9
13. Waschkies CF, Bruns A, Müller S, Kapps M, Borroni E, Von Kienlin M, et al. Neuropharmacological and Neurobiological Relevance of In vivo 1H-MRS of GABA and Glutamate for Preclinical Drug Discovery in Mental Disorders. Neuropsychopharmacology. 2014;39:2331–9. https://doi.org/10.1038/npp.2014.79
14. Petroff OAC. GABA and Glutamate in the Human Brain. Neuroscientist. 2002;8:562–73. https://doi.org/10.1177/1073858402238515
15. Pellerin L, Magistretti PJ. Glutamate uptake into astrocytes stimulates aerobic glycolysis: a mechanism coupling neuronal activity to glucose utilization. Proc Natl Acad Sci USA. 1994;91:10625–9. https://doi.org/10.1073/pnas.91.22.10625
16. Frye RE. Mitochondrial Dysfunction in Autism Spectrum Disorder: Unique Abnormalities and Targeted Treatments. Semin Pediatr Neurol. 2020;35:100829. https://doi.org/10.1016/j.spen.2020.100829
17. Rossignol DA, Frye RE. Mitochondrial dysfunction in autism spectrum disorders: a systematic review and meta-analysis. Mol Psychiatry. 2012;17:290–314. https://doi.org/10.1038/mp.2010.136
18. Brand A, Richter-Landsberg C, Leibfritz D. Multinuclear NMR studies on the energy metabolism of glial and neuronal cells. Dev Neurosci. 1993;15:289–98. https://doi.org/10.1159/000111347
19. Goh S, Dong Z, Zhang Y, DiMauro S, Peterson BS. Mitochondrial Dysfunction as a Neurobiological Subtype of Autism Spectrum Disorder: Evidence From Brain Imaging. JAMA Psychiatry. 2014;71:665–71. https://doi.org/10.1001/jamapsychiatry.2014.179
20. Maier S, Nickel K, Lange T, Oeltzschner G, Dacko M, Endres D, et al. Increased cerebral lactate levels in adults with autism spectrum disorders compared to non-autistic controls: a magnetic resonance spectroscopy study. Mol Autism. 2023;14:44. https://doi.org/10.1186/s13229-023-00577-y
21. Cochran DM, Sikoglu EM, Hodge SM, Edden RAE, Foley A, Kennedy DN, et al. Relationship among Glutamine, γ-Aminobutyric Acid, and Social Cognition in Autism Spectrum Disorders. J Child Adolesc Psychopharmacol. 2015;25:314–22. https://doi.org/10.1089/cap.2014.0112
22. Oya M, Matsuoka K, Kubota M, Fujino J, Tei S, Takahata K, et al. Increased glutamate and glutamine levels and their relationship to astrocytes and dopaminergic transmissions in the brains of adults with autism. Sci Rep. 2023;13:11655. https://doi.org/10.1038/s41598-023-38306-3
23. Tebartz van Elst L, Maier S, Fangmeier T, Endres D, Mueller GT, Nickel K, et al. Disturbed cingulate glutamate metabolism in adults with high-functioning autism spectrum disorder: evidence in support of the excitatory/inhibitory imbalance hypothesis. Mol Psychiatry. 2014;19:1314–25. https://doi.org/10.1038/mp.2014.62
24. Shimmura C, Suzuki K, Iwata Y, Tsuchiya KJ, Ohno K, Matsuzaki H, et al. Enzymes in the glutamate-glutamine cycle in the anterior cingulate cortex in postmortem brain of subjects with autism. Mol Autism. 2013;4:6. https://doi.org/10.1186/2040-2392-4-6
25. Zhang H, Schneider T, Wheeler-Kingshott CA, Alexander DC. NODDI: Practical *in vivo* neurite orientation dispersion and density imaging of the human brain. NeuroImage. 2012;61:1000–16. https://doi.org/10.1016/j.neuroimage.2012.03.072
26. Choi DW. Excitotoxic cell death. J Neurobiol. 1992;23:1261–76. https://doi.org/10.1002/neu.480230915
27. Courchesne E, Pierce K. Brain overgrowth in autism during a critical time in development: implications for frontal pyramidal neuron and interneuron development and connectivity. Int J Dev Neurosci. 2005;23:153–70. https://doi.org/10.1016/j.ijdevneu.2005.01.003
28. Kato TA, Suzuki Y, Horie K, Teo AR, Sakamoto S. One month version of Hikikomori Questionnaire-25 (HQ-25M): development and initial validation [Letter]. Psychiatry Clin Neurosci. 2023;77:188–9. https://doi.org/10.1111/pcn.13499
29. Kato TA, Kanba S, Teo AR. Hikikomori: multidimensional understanding, assessment, and future international perspectives. Psychiatry Clin Neurosci. 2019;73:427–40. https://doi.org/10.1111/pcn.12895

30. Yamada M, Kato TA, Katsuki RI, Yokoi H, Igarashi M, Komine Y, et al. Pathological social withdrawal in autism spectrum disorder: A case control study of hikikomori in Japan. Front Psychiatry. 2023;14:1114224. https://doi.org/10.3389/fpsyt.2023.1114224
31. Muris P, van der Veen A, Luijten B, De Bie C, Meesters C. On Your Own: An Explorative Study on the Psychopathological and Psychosocial Correlates of Hikikomori Symptoms in Dutch Adolescents and Young Adults. Child Psychiatry Hum Dev. 2025; https://doi.org/10.1007/s10578-025-01828-0
32. Teo AR, Chen JI, Kubo H, Katsuki R, Sato-Kasai M, Shimokawa N, et al. Development and validation of the 25-item Hikikomori Questionnaire (HQ-25). Psychiatry Clin Neurosci. 2018;72:780–8. https://doi.org/10.1111/pcn.12691
33. Komori T, Okamura K, Ikehara M, Yamamuro K, Endo N, Okumura K, et al. Brain-derived neurotrophic factor from microglia regulates neuronal development in the medial prefrontal cortex and its associated social behavior. Mol Psychiatry. 2024;29:1338–49. https://doi.org/10.1038/s41380-024-02413-y
34. American Psychiatric Association. Diagnostic and Statistical Manual of Mental Disorders. 5th ed. Arlington, VA: American Psychiatric Publishing; 2013.
35. Lord C, Risi S, Lambrecht L, Cook EH, Leventhal BL, DiLavore PC, et al. The Autism Diagnostic Observation Schedule—Generic: A Standard Measure of Social and Communication Deficits Associated with the Spectrum of Autism. J Autism Dev Disord. 2000;30:205–23. https://doi.org/10.1023/A:1005592401947
36. Pugliese CE, Kenworthy L, Bal VH, Wallace GL, Yerys BE, Maddox BB, et al. Replication and Comparison of the Newly Proposed ADOS-2, Module 4 Algorithm in ASD Without ID: A Multi-site Study. J Autism Dev Disord. 2015;45:3919–31. https://doi.org/10.1007/s10803-015-2586-3
37. Otsubo T, Tanaka K, Koda R, Shinoda J, Sano N, Tanaka S, et al. Reliability and validity of Japanese version of the Mini-International Neuropsychiatric Interview. Psychiatry Clin Neurosci. 2005;59:517–26. https://doi.org/10.1111/j.1440-1819.2005.01408.x
38. Sattler JM. Assessment of Children: Cognitive Foundations. J.M. Sattler; 2008.
39. Wakabayashi A, Baron-Cohen S, Wheelwright S, Tojo Y. The Autism-Spectrum Quotient (AQ) in Japan: A Cross-Cultural Comparison. J Autism Dev Disord. 2006;36:263–70. https://doi.org/10.1007/s10803-005-0061-2
40. Baron-Cohen S, Wheelwright S, Skinner R, Martin J, Clubley E. The Autism-Spectrum Quotient (AQ): Evidence from Asperger Syndrome/High-Functioning Autism, Males and Females, Scientists and Mathematicians. J Autism Dev Disord. 2001;31:5–17. https://doi.org/10.1023/A:1005653411471
41. Hirata K, Matsuoka K, Tagai K, Endo H, Tatebe H, Ono M, et al. Altered Brain Energy Metabolism Related to Astrocytes in Alzheimer's Disease. Ann Neurol. 2024;95:104–15. https://doi.org/10.1002/ana.26797
42. Matsuoka K, Takado Y, Tagai K, Kubota M, Sano Y, Takahata K, et al. Two pathways differentially linking tau depositions, oxidative stress, and neuronal loss to apathetic phenotypes in progressive supranuclear palsy. J Neurol Sci. 2023;444:120514. https://doi.org/10.1016/j.jns.2022.120514
43. Mekle R, Mlynárik V, Gambarota G, Hergt M, Krueger G, Gruetter R. MR spectroscopy of the human brain with enhanced signal intensity at ultrashort echo times on a clinical platform at 3T and 7T. Magn Reson Med. 2009;61:1279–85. https://doi.org/10.1002/mrm.21961
44. Simpson R, Devenyi GA, Jezzard P, Hennessy TJ, Near J. Advanced processing and simulation of MRS data using the FID appliance (FID-A)-An open source, MATLAB-based toolkit. Magn Reson Med. 2017;77:23–33. https://doi.org/10.1002/mrm.26091
45. Provencher SW. Estimation of metabolite concentrations from localized in vivo proton NMR spectra. Magn Reson Med. 1993;30:672–9. https://doi.org/10.1002/mrm.1910300604
46. Provencher SW. Automatic quantitation of localized in vivo ^{1}H spectra with LCModel. NMR Biomed. 2001;14:260–4. https://doi.org/10.1002/nbm.698
47. Harris AD, Puts NAJ, Edden RAE. Tissue correction for GABA-edited MRS: considerations of voxel composition, tissue segmentation and tissue relaxations. J Magn Reson Imaging. 2015;42:1431–40. https://doi.org/10.1002/jmri.24903

48. Dhamala E, Abdelkefi I, Nguyen M, Hennessy TJ, Nadeau H, Near J. Validation of *in vivo* MRS measures of metabolite concentrations in the human brain. NMR Biomed. 2019;32:e4058. https://doi.org/10.1002/nbm.4058
49. Wyss PO, Bianchini C, Scheidegger M, Giapitzakis IA, Hock A, Fuchs A, et al. In vivo estimation of transverse relaxation time constant (T2) of 17 human brain metabolites at 3T. Magn Reson Med. 2018;80:452–61. https://doi.org/10.1002/mrm.27067
50. Zhang Y, Brady M, Smith S. Segmentation of brain MR images through a hidden Markov random field model and the expectation-maximization algorithm. IEEE Trans Med Imaging. 2001;20:45–57. https://doi.org/10.1109/42.906424
51. Lin A, Andronesi O, Bogner W, Choi I, Coello E, Cudalbu C, et al. Minimum Reporting Standards for in vivo Magnetic Resonance Spectroscopy (MRSinMRS): Experts' consensus recommendations. NMR Biomed. 2021;34:e4484. https://doi.org/10.1002/nbm.4484
52. Smith SM, Jenkinson M, Woolrich MW, Beckmann CF, Behrens TEJ, Johansen-Berg H, et al. Advances in functional and structural MR image analysis and implementation as FSL. Neuroimage. 2004;23:S208–19. https://doi.org/10.1016/j.neuroimage.2004.07.051
53. Andersson JLR, Skare S, Ashburner J. How to correct susceptibility distortions in spin-echo echo-planar images: application to diffusion tensor imaging. Neuroimage. 2003;20:870–88. https://doi.org/10.1016/S1053-8119(03)00336-7
54. Andersson JLR, Sotiropoulos SN. An integrated approach to correction for off-resonance effects and subject movement in diffusion MR imaging. Neuroimage. 2016;125:1063–78. https://doi.org/10.1016/j.neuroimage.2015.10.019
55. Epskamp S, Fried E. A Tutorial on Regularized Partial Correlation Networks. Psychol Methods. 2018;23:617–34. https://doi.org/10.1037/met0000167
56. Hagihara H, Catts VS, Katayama Y, Shoji H, Takagi T, Huang FL, et al. Decreased Brain pH as a Shared Endophenotype of Psychiatric Disorders. Neuropsychopharmacology. 2018;43:459–68. https://doi.org/10.1038/npp.2017.167
57. Goji A, Ito H, Mori K, Harada M, Hisaoka S, Toda Y, et al. Assessment of Anterior Cingulate Cortex (ACC) and Left Cerebellar Metabolism in Asperger's Syndrome with Proton Magnetic Resonance Spectroscopy (MRS). PLoS One. 2017;12:e0169288. https://doi.org/10.1371/journal.pone.0169288
58. Aoki Y, Kasai K, Yamasue H. Age-related change in brain metabolite abnormalities in autism: a meta-analysis of proton magnetic resonance spectroscopy studies. Transl Psychiatry. 2012;2:e69. https://doi.org/10.1038/tp.2011.65
59. Gatto RG, Mustafi SM, Amin MY, Mareci TH, Wu Y-C, Magin RL. Neurite orientation dispersion and density imaging can detect presymptomatic axonal degeneration in the spinal cord of ALS mice. Funct Neurol. 2018;33:155–63.
60. Yi SY, Barnett BR, Torres-Velázquez M, Zhang Y, Hurley SA, Rowley PA, et al. Detecting Microglial Density With Quantitative Multi-Compartment Diffusion MRI. Front Neurosci. 2019;13:81. https://doi.org/10.3389/fnins.2019.00081
61. Takada R, Toritsuka M, Yamauchi T, Ishida R, Kayashima Y, Nishi Y, et al. Granulocyte macrophage colony-stimulating factor-induced macrophages of individuals with autism spectrum disorder adversely affect neuronal dendrites through the secretion of pro-inflammatory cytokines. Mol Autism. 2024;15:10. https://doi.org/10.1186/s13229-024-00589-2
62. Lombardo MV, Lai M-C, Baron-Cohen S. Big data approaches to decomposing heterogeneity across the autism spectrum. Mol Psychiatry. 2019;24:1435–50. https://doi.org/10.1038/s41380-018-0321-0
63. Rose S, Niyazov DM, Rossignol DA, Goldenthal M, Kahler SG, Frye RE. Clinical and Molecular Characteristics of Mitochondrial Dysfunction in Autism Spectrum Disorder. Mol Diagn Ther. 2018;22:571–93. https://doi.org/10.1007/s40291-018-0352-x
64. Casanova MF, Shaban M, Ghazal M, El-Baz AS, Casanova EL, Opris I, et al. Effects of Transcranial Magnetic Stimulation Therapy on Evoked and Induced Gamma Oscillations in Children with Autism Spectrum Disorder. Brain Sci. 2020;10:423. https://doi.org/10.3390/brainsci10070423
65. Casanova MF, Sokhadze EM, Casanova EL, Opris I, Abujadi C, Marcolin MA, et al. Translational Neuroscience in Autism. Psychiatr Clin North Am. 2020;43:229–48. https://doi.org/10.1016/j.psc.2020.02.004
66. Moxon-Emre I, Daskalakis ZJ, Blumberger DM, Croarkin PE, Lyon RE, Forde NJ, et al. Modulation of Dorsolateral Prefrontal Cortex Glutamate/Glutamine Levels Following Repetitive Transcranial Magnetic Stimulation in Young Adults With Autism.

Front Neurosci. 2021;15:711542. https://doi.org/10.3389/fnins.2021.711542

67. Michael N, Gösling M, Reutemann M, Kersting A, Heindel W, Arolt V, et al. Metabolic changes after repetitive transcranial magnetic stimulation (rTMS) of the left prefrontal cortex: a sham-controlled proton magnetic resonance spectroscopy (1H MRS) study of healthy brain. Eur J Neurosci. 2003;17:2462–8. https://doi.org/10.1046/j.1460-9568.2003.02683.x
68. Ge R, Downar J, Blumberger DM, Daskalakis ZJ, Vila-Rodriguez F. Functional connectivity of the anterior cingulate cortex predicts treatment outcome for rTMS in treatment-resistant depression at 3-month follow-up. Brain Stimul. 2020;13:206–14. https://doi.org/10.1016/j.brs.2019.10.012
69. Cao H, Zuo C, Gu Z, Huang Y, Yang Y, Zhu L, et al. High frequency repetitive transcranial magnetic stimulation alleviates cognitive deficits in 3xTg-AD mice by modulating the PI3K/Akt/GLT-1 Axis. Redox Biol. 2022;54:102354. https://doi.org/10.1016/j.redox.2022.102354
70. Al-Ghabban H, Bashiri FA, Alenezi S, El-Ansary A, Sabr A, Alayadhi L. Therapeutic potential of low-frequency transcranial magnetic stimulation in children with autism spectrum disorder: sensory and behavioral outcomes—a randomized trial. Front Psychiatry. 2026;17:1725598. https://doi.org/10.3389/fpsyt.2026.1725598

Figures

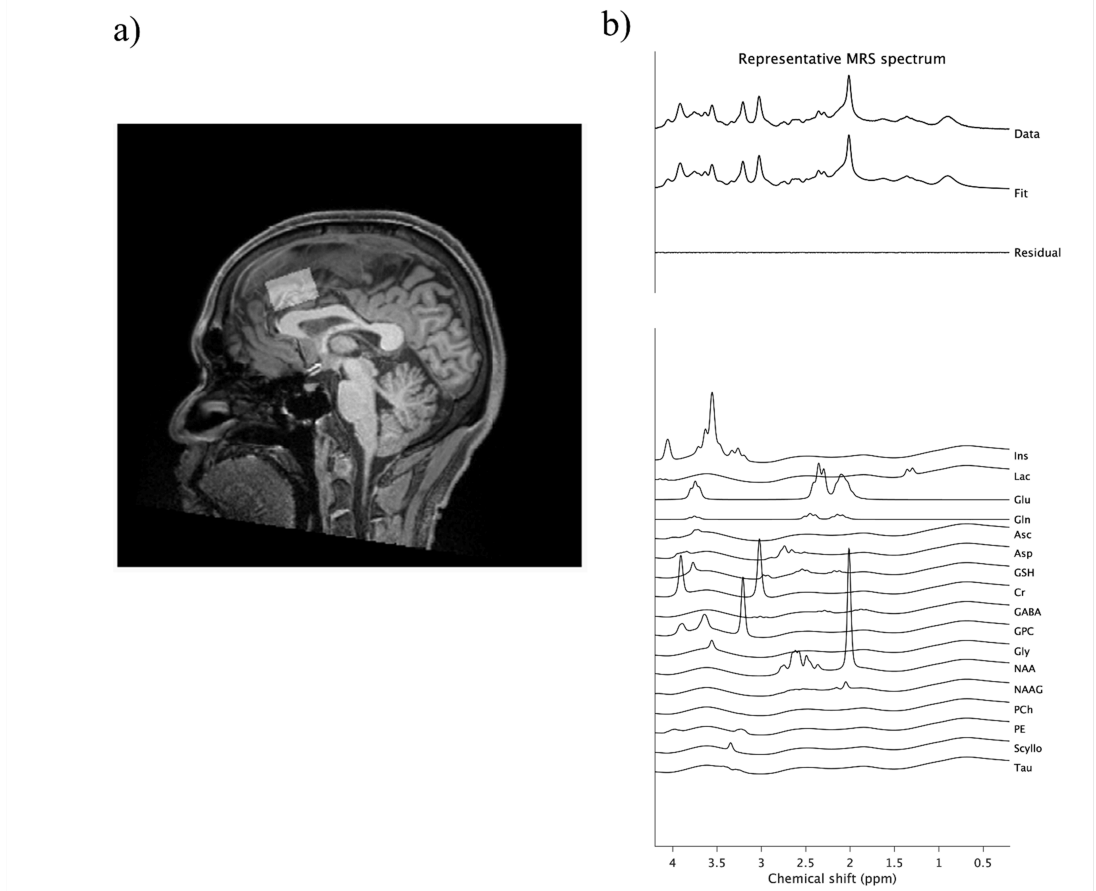


Figure 1

Representative voxel of interest (VOI) and MRS spectrum in an adult with ASD.

(a) VOI (30 × 20 × 20 mm³) placed in the anterior cingulate cortex (ACC) of an adult with ASD. (b) Representative ¹H-MRS spectrum with LCModel fit, individual metabolite fits, and residual. ACC, anterior cingulate cortex; VOI, voxel of interest; MRS, magnetic resonance spectroscopy.

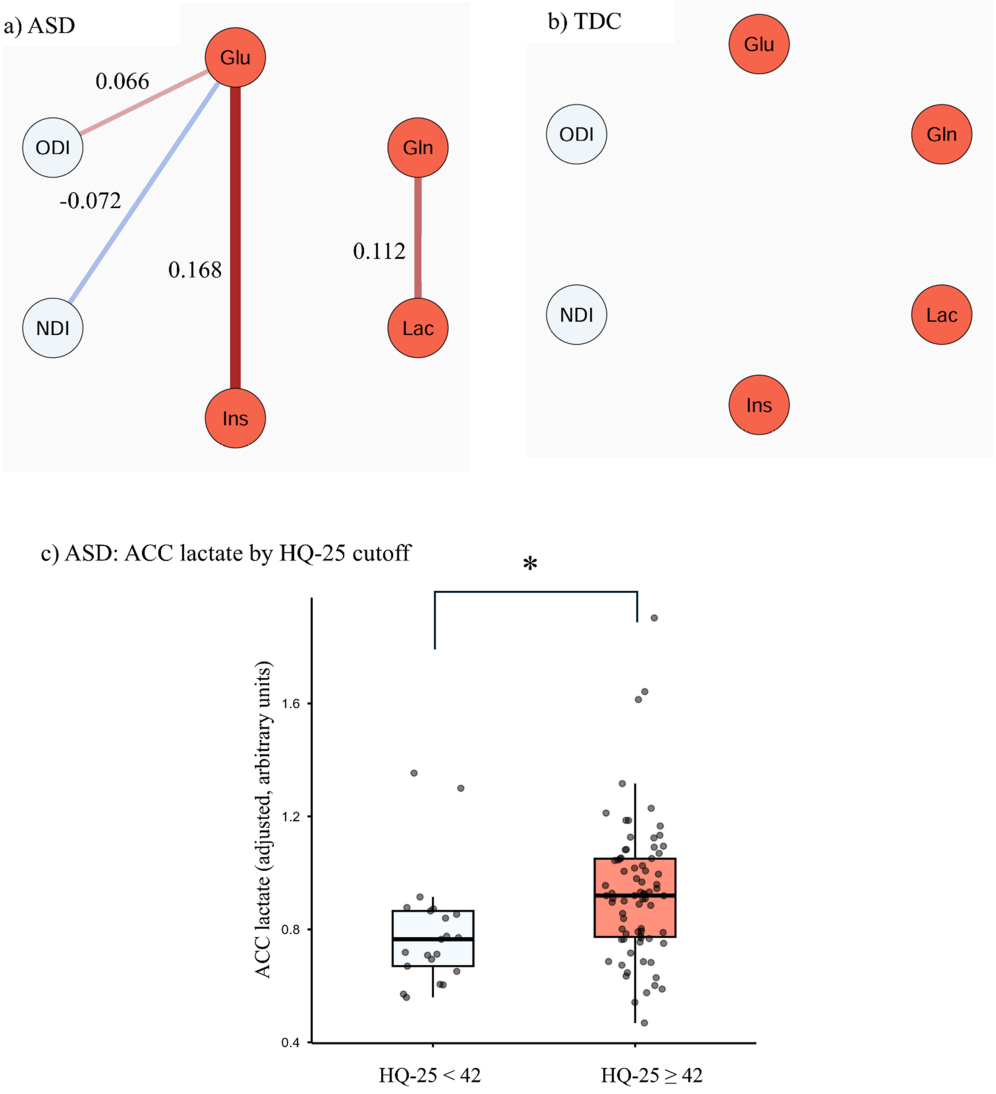


Figure 2

Figure 2

ACC metabolic–microstructural networks in ASD and TDC, and ACC lactate by social withdrawal status in ASD.

(a, b) Partial correlation networks (EBICglasso, γ = 0.25) of ACC metabolites (red nodes: Glu, Gln, Lac, Ins) and NODDI indices (white nodes: NDI, ODI) in ASD (a) and TDC (b), adjusted for age, sex, and estimated FSIQ. Edge width indicates the strength of partial Spearman correlations (red, positive; blue, negative), and numbers are edge weights. No edges were retained in TDC (b). Node layout is identical in (a) and (b). (c) ACC Lac in participants with ASD below (HQ-25 < 42, n = 19) and at or above (HQ-25 ≥ 42, n = 77) the HQ-25 cutoff. Boxes show the median and interquartile range, whiskers extend to 1.5 times the

interquartile range, and dots are individual participants. *p = 0.014 (permutation ANCOVA adjusted for age, sex, and estimated FSIQ).

Abbreviations: ACC, anterior cingulate cortex; ANCOVA, analysis of covariance; ASD, autism spectrum disorder; EBICglasso, graphical lasso with extended Bayesian information criterion; FSIQ, full-scale intelligence quotient; Gln, glutamine; Glu, glutamate; HQ-25, 25-item Hikikomori Questionnaire; Ins, myo-inositol; Lac, lactate; NDI, neurite density index; NODDI, neurite orientation dispersion and density imaging; ODI, orientation dispersion index; TDC, typically developing controls.

Supplementary Files

This is a list of supplementary files associated with this preprint. Click to download.

- SupplementaryFigure1.tif
- SupplementaryInformation2.docx